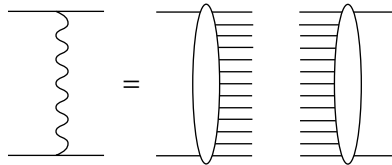# 15
Particle density fluctuations and RFT

15.1 Reggeon branchings and AGK cutting rules

15.1.1 Inelastic processes corresponding to reggeon branchings

In this lecture we will investigate the correspondence between various inelastic processes and reggeon diagrams. We begin with the simplest object, the pole.


As before, we assume an essential property, namely: that the particle distribution emerging from cutting the pomeron pole is *homogeneous*, i.e. the inclusive spectrum $\varphi(k_\perp^2)$ does not depend on the rapidity η:

$$\frac{d^3\sigma}{d\eta\, d^2\mathbf{k}_\perp} = g_1 G(\xi - \eta)\varphi G(\eta)g_2 = \sigma_{\text{tot}} \cdot \varphi(k_\perp^2). \qquad (15.1)$$
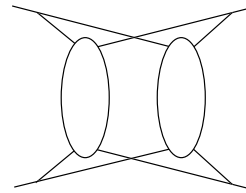
For $\xi - \eta \sim 1$ $(\eta \sim 1)$ when the particle is close in rapidity to one of the fragmentation regions, the shape of the particle yield depends on the

381

quantum numbers of the registered particle and of the projectile (target):
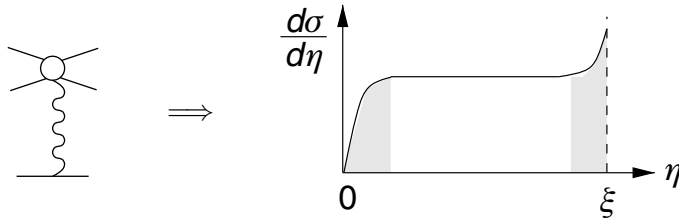
If each pole corresponds to the uniform distribution, what sort of inelastic processes are contained in the branching of two such poles?

In Lecture 12 we have calculated the two-reggeon branching diagram as a whole. Now I would like to find out, what sort of imaginary parts it has; in other words, how can the diagram be cut?

(1) First of all, we can have a quasi-elastic process by making a cut between the reggeons:

$$(15.2a)$$
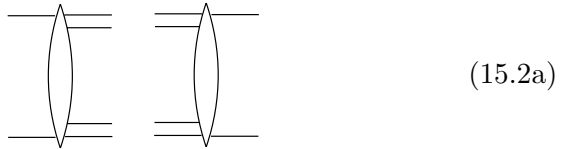
(2) One can cut one of the two ladders:

$$(15.2b)$$
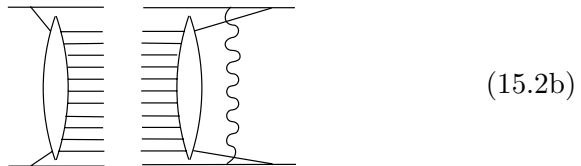
which gives the correction to the probability of having the usual final particle distribution.

(3) Finally, both ladders can be cut:

$$(15.2c)$$

I get two new processes, (1) and (3), in addition to the correction (2). In case (3) I observe two ladders at the same time, i.e. the particle density is twice as high as before. So, the branching describes fluctuations of the number of final state particles.

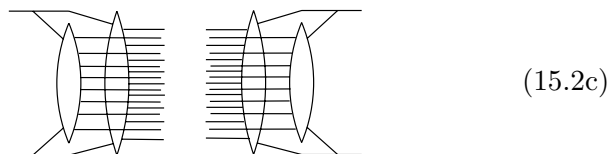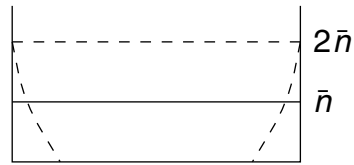Curiously, the changes are rather sharp – there is either no particle in the plateau region, or a 100% enhancement. Obviously, we have chosen too simple a diagram.

By taking enhanced diagrams, we obtain various *local* fluctuations. For example, by cutting the two-pomeron loop in the Green function, we get:

(1) a central rapidity gap;

$$\text{(15.3a)}$$
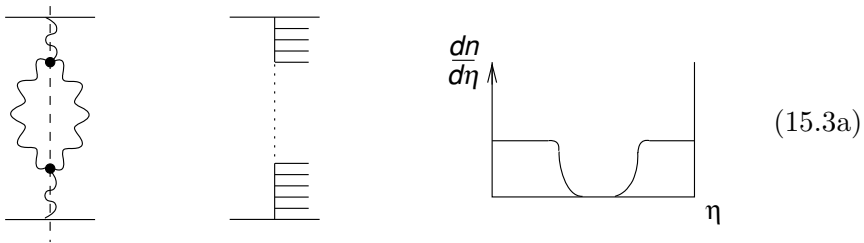
(2) another correction to the uniform ladder;

$$\text{(15.3b)}$$
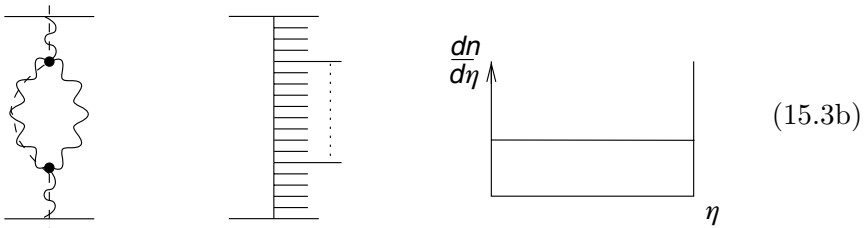
(3) a local double density fluctuation.

$$\text{(15.3c)}$$
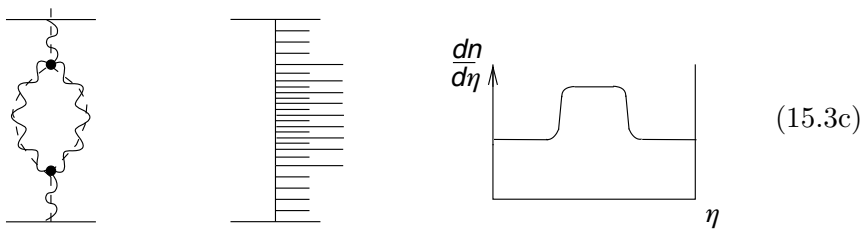
Considering a diagram with three reggeons in the *t*-channel, we will have *triple particle density* as a new fluctuation (plus extra corrections to the distributions that we already had).

From the point of view of the *s*-channel, the self-consistency of our picture implies moderate fluctuations in the particle density. Recall an analogy with 'particle gas' that we have discussed in Lecture 10. A statistical system is stable when fluctuations are small. On the other hand, we are near the critical point where fluctuations of arbitrary size emerge. As we already know, the weak coupling corresponds to small fluctuations. In the strong coupling regime, on the contrary, fluctuations are large, so large that there is no average density at all.

Not having solved the interacting pomeron theory, we do not know how to cut the exact Green function; and this is the problem. In spite of this, it turns out to be possible to understand the pattern of fluctuations in multi-particle production that is induced by the presence of pomeron branchings.
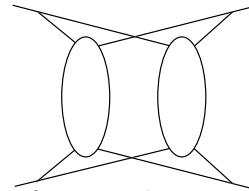
15.1.2 Two-reggeon branching

Let us study the two-reggeon branching diagram, $F^{(2)}$. Now I will be interested not in the expression for $\mathrm{Im}_s\, F^{(2)}$ itself, but what processes it is assembled from. We have to learn to extract such an information from our knowledge of the expression for the diagram as a whole.

Recall that at high energies the amplitude became factorized,

$$\frac{d^4k}{(2\pi)^4\,i} \to i\cdot\frac{d^2\mathbf{k}_\perp}{(2\pi)^2}\cdot\frac{d\alpha}{2\pi i}\frac{d\beta}{2\pi\,i},$$

integrals over α and β produced real particle–reggeon vertex functions, N, on the top and the bottom of the diagram, and left us with a factor i for the reggeon loop. So, the branching can be written as

$$F^{(2)} = N\cdot f_1\,if_2\cdot N, \tag{15.4}$$

with f the reggeon amplitude. This expression is symbolic; integration over $d^2\mathbf{k}$ is implied. However, it represents correctly the nature of the complexity of the amplitude.

It is convenient to calculate the double imaginary part (discontinuity), $2\,\mathrm{Im}$. Then the calculation reduces to putting all cut particles on mass shell by replacing their propagators by delta-fuctions, e.g.

$$2\,\mathrm{Im}\int\frac{d^4\ell}{(2\pi)^4\,i}\frac{1}{m^2-\ell^2}\frac{1}{m^2-(P-\ell)^2}=\int\frac{d^4\ell}{(2\pi)^2}\delta(m^2-\ell^2)\delta(m^2-(P-\ell)^2).$$

Let us see how our diagram can be cut.

(1) The simplest imaginary part arises from cutting *between* the reggeons and corresponds to quasi-elastic scattering:

$$2\,\mathrm{Im}^{(1)}F^{(2)} \;=\; N^2\big(f_1 f_2^* + f_1^* f_2\big) \;=\; 2N^2|f|^2\,. \qquad (15.5\mathrm{a})$$
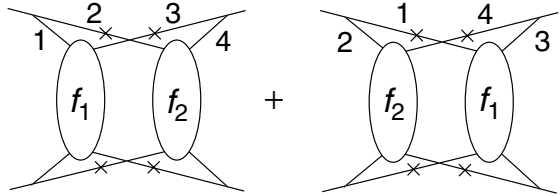
(2) We may cut through one reggeon, say, f_1. The second one may then stand either on the left from the cut (and describe rescattering of particle 2 in the amplitude) or on the right (rescattering in the conjugated amplitude),

$$2\,\mathrm{Im}F^{(2)} \Longrightarrow 2\,\mathrm{Im}\,f_1 \cdot \big(if_2 + (if_2)^*\big).$$

We have to add the cut through f_2 (and rescattering of particle 1):

$$2\,\mathrm{Im}^{(2)}F^{(2)} = N^2\big[2\,\mathrm{Im}f_1\big(if_2 + (if_2)^*\big) + 2\,\mathrm{Im}\,f_2\big(if_1 + (if_1)^*\big)\big]$$
$$= -8N^2(\mathrm{Im}\,f)^2. \qquad (15.5\mathrm{b})$$

(3) What remains to be done is simple: the last cut has to be made through both blocks, replacing all particle propagators inside the reggeon 'ladders' by delta functions:

$$2\,\mathrm{Im}^{(3)}F^{(2)} \;=\; N^2 \cdot 2\,\mathrm{Im}\,f_1 \cdot 2\,\mathrm{Im}\,f_2 \;=\; 4N^2(\mathrm{Im}\,f)^2. \qquad (15.5\mathrm{c})$$

Adding together (15.5), we obtain the imaginary part of the branching as consisting of three pieces,

$$2\,\mathrm{Im}_s F^{(2)} = N^2\big[2ff^* - 8(\mathrm{Im}\,f)^2 + 4(\mathrm{Im}\,f)^2\big]. \qquad (15.6)$$

We may verify our conclusion by directly evaluating the imaginary part of the symbolic expression (15.4):

$$2\,\mathrm{Im}\,F^{(2)} = 2\,\mathrm{Im}\,\big\{NfifN\big\} = 2N^2\,\mathrm{Re}\,f^2 = 2N^2\big\{(\mathrm{Re}\,f)^2 - (\mathrm{Im}\,f)^2\big\}$$
$$= 2N^2[ff^* - 2(\mathrm{Im}\,f)^2] \equiv N^2\big[2ff^* - 8(\mathrm{Im}\,f)^2 + 4(\mathrm{Im}\,f)^2\big].$$

The first and third terms in the r.h.s. of (15.6) are positive because they represent cross sections of two processes: quasi-diffractive scattering and double density particle production. The second term is a correction to the
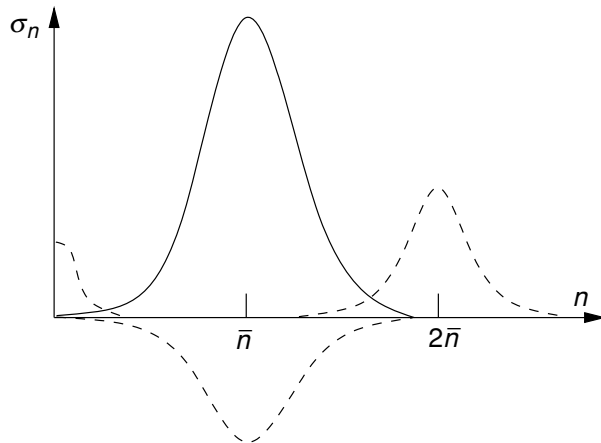
Fig. 15.1 Topological cross section distribution corresponding to single pomeron (solid line) and multiplicity fluctuation pattern induced by two-pomeron branching (dashed).

pole; it may be negative (though not very). The relation $2 : 8 : 4$ expresses the share of different final states contained in the imaginary part.

This simple example illustrates an important pattern of fluctuations in the multiplicity distribution induced by branchings. The cross section in the main region, $n \sim \bar{n}$, *decreases* (-8) to make room for the new particle production processes (characterized by the shares $+2$ and $+4$) as shown in Fig. 15.1. For the pomeron pole we have $|\operatorname{Re} f| \ll \operatorname{Im} f$, so that

$$2 \operatorname{Im}_s F \simeq N^2 (2 - 8 + 4)(\operatorname{Im} f)^2 = -2N^2 (\operatorname{Im} f)^2. \tag{15.7}$$

The overall effect of the branching is *negative*; the total cross section decreases. This is screening.

This is an example of how we can sort out the content of $\operatorname{Im}_s F$ of arbitrary multi-reggeon diagrams. It is important that we did so according to the cuts of f, not touching N. This means that the we have carried the procedure in a universal way, and did not need to worry about the (potentially complicated) internal structure of the vertices.

15.1.3 Universality of the vertex function N

In the derivation we implied only one (but essential) thing, namely that the vertex block N remains the same in all cases (15.5). I would prove that the expression (15.6) is correct if N, indeed, does not depend on the way we cut the diagram.

To see that this is indeed the case, let me remind you what we did before. We expressed all particle momenta in terms of Sudakov variables using the momentum vectors p_1, p_2 of colliding particles as

$$k_i^\mu = \alpha_i p_1^\mu + \beta_i p_2^\mu + k_{i\perp}^\mu.$$

In the upper part of the graph, close to p_1, we have $\alpha_i \sim 1$, $\beta_i \sim 1/s$. The small components, β_i, do not affect the lower part of the diagram and hence, the β_i-integrations concern only the upper vertex block,

$$\text{(15.8)}$$
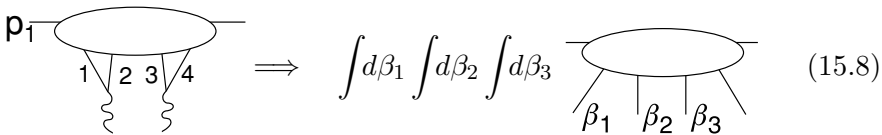
Recall

$$s_1 = (p_1 + k_1)^2 = (1 + \alpha_1)(\gamma + \beta_1)s \implies s\,d\beta_1 = ds_1.$$

This shows that the block is integrated over the invariant energies (because of energy–momentum conservation, there are three independent integrations). The integration reduces to the closing of the contour around the physical cut and thus to the transition to real states:
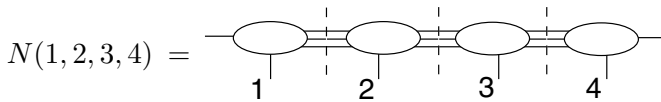
In fact, after integration over energies the function N becomes symmetric with respect to the transmutation of particles 1, 2, 3, 4. I said that to cut the diagram means to make a certain set of internal particles real. But inside the block N all particles are already on the mass shell; it can be treated as a real function, in a deep sense: there is no way to cut it any further.

To clarify this important point, let us imagine that external particles are represented by operators of some field theory. Then the function N is given by the time-product

$$A(k_i) = \int \langle p_1' | T \varphi_1(x_1)\varphi_2(x_2)\varphi_3(x_3)\varphi_4(0) | p_1 \rangle \prod_{i=1}^{3} \mathrm{e}^{ik_i x_i}\,d^4 x_i\,. \qquad \text{(15.9)}$$

As we have already seen, this expression does not itself enter our calculations, just its integral over all energies:

$$N = \int dk_{10} \int dk_{20} \int dk_{30}\,A.$$

It gives $\delta(t_1)\delta(t_2)\delta(t_3)$, so that the time ordering sign, T, can be omitted and we obtain an equal-time product of *commuting* operators,

$$N = \int \langle |\varphi_1(\mathbf{r}_1,0)\varphi_2(\mathbf{r}_2,0)\varphi_3(\mathbf{r}_3,0)\varphi_4(0,0)| \rangle \prod_{i=1}^{3} e^{-i\mathbf{k}_i \cdot \mathbf{r}_i}\, d^3\mathbf{r}_i.$$

This expression can be written in terms of real intermediate states, in various equivalent ways. In particular,
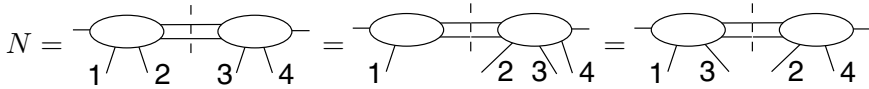
In the notation of (15.8), the first representation enters the quasi-diffractive imaginary part (15.5a), the second – (one of the four) one-reggeon cuts (15.5b), and the third – the cut through both pomerons (15.5c).

From our derivation it is clear that this property applies to particle–reggeon blocks with an arbitrary number of reggeons attached. It also holds for reggeon–reggeon interactions, like the three-reggeon vertices r in the enhanced correction graph (15.3).

Now we will generalize the result (15.4),

$$F^{(2)} \sim N \cdot f\,i\,f \cdot N,$$

to multi-reggeon branchings. Astonishing cancellations will allow us to calculate *inclusive particle spectra* in the most general manner, even for the case of strong coupling.

15.1.4 Cutting through many reggeons

What happens in multi-reggeon branchings? Let us write, in analogy with the two-reggeon case, (15.4),

$$= N_{(n)} \underbrace{f\,i\,f\,i\ldots i\,f}_{n} N_{(n)}. \qquad (15.10)$$

In the same way as before, the particle–reggeon vertices $N_{(n)}$ do not change when we cut the diagram. What is the contribution to different processes of a non-enhanced n-reggeon diagram with n_1 cut reggeons? This is a simple combinatorial problem. We put n_2 uncut reggeons on the left of the cut ones, and the remaining $n - n_1 - n_2$ on the right, as shown
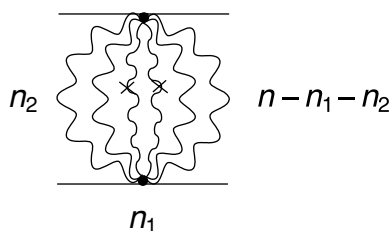
Fig. 15.2 *n*-reggeon diagram with n_1 cut reggeons.

in Fig. 15.2, and write

$$2\operatorname{Im} F^{(n)}_{n_1,n_2} = N^2_{(n)} (2\operatorname{Im} f)^{n_1} (if)^{n_2} (-if^*)^{n-n_1-n_2} C^{n_1}_n C^{n_2}_{n-n_1}. \quad (15.11)$$

The combinatorial factors C count the number of ways to choose n_1 cut reggeons from n, and to divide $n - n_1$ uncut ones into n_2 to be put into the amplitude (left) and $n - n_1 - n_2$ into the amplitude conjugate; $C^k_m = m!/k!(m-k)!$. We are interested in the sum over n_2:

$$\sum_{n_2=0}^{n-n_1} C^{n_2}_{n-n_1}(if)^{n_2}(-if^*)^{n-n_1-n_2} = (if - if^*)^{n-n_1} = (-1)^{n-n_1}(2\operatorname{Im} f)^{n-n_1}.$$

Substituting into (15.11) yields the contribution to the cross section with n_1 cut reggeons ($n_1 \geq 1$):

$$2\operatorname{Im} F^{(n)}_{n_1} = \sum_{n_2} 2\operatorname{Im} F^{(n)}_{n_1,n_2} = (-1)^{n-n_1} C^{n_1}_n (2\operatorname{Im} f)^n N^2_{(n)}. \quad (15.12)$$

We have to consider the case when no reggeon is cut ($n_1 = 0$) separately. To this end we calculate the number of ways to split n reggeons into $n_2 \geq 1$ to the left of the cut (with $n - n_2 \geq 1$ to the right), and take the imaginary part of the factor i separating the two groups in (15.10),

$$\sum_{n_2=1}^{n-1} (if)^{n_2}((if)^*)^{n-n_2} C^{n_2}_n = \underbrace{(if - if^*)^n}_{(-2\operatorname{Im} f)^n} - (if)^n - ((if)^*)^n,$$

producing

$$2\operatorname{Im} F^{(n)}_0 = (-1)^n (2\operatorname{Im} f)^n N_{(n)} - 2\operatorname{Re}[(if)^n] N_{(n)}. \quad (15.13)$$

Adding together (15.12) and (15.13) we have

$$\sum_{n_1=0}^{n} C^{n_1}_n (-1)^{n_1} \cdot (-2\operatorname{Im} f)^n - 2\operatorname{Re}[(if)^n] = -2\operatorname{Re}[(if)^n],$$

since the sum equals zero $((1+x)^n|_{x=-1})$. Thus, for the total imaginary part we obtain

$$2\operatorname{Im}F^{(n)} = -2\operatorname{Re}(if)^n N_{(n)}^2 = 2\operatorname{Im}\big[-i(if)^n\big]N_{(n)}^2,$$

in agreement with (15.10).

Let us note that in the case of $n=2$, from (15.13) ($n_1 = 0$) and (15.12) ($n_1 = 1, 2$) we rederive the known proportion (15.7):

$$\operatorname{Im}F_0^{(2)} : \operatorname{Im}F_1^{(2)} : \operatorname{Im}F_2^{(2)} \ = \ 2 : -8 : 4.$$

Thus, a simple calculation gave us an important result for the composition of the n-reggeon branching: the contribution to the cross section with n_1 cut reggeons, $0 \le n_1 \le n$, is

$$2\operatorname{Im}_s F_{n_1}^{(n)} = \big((-1)^{n-n_1}C_n^{n_1}(2\operatorname{Im}f)^n - 2\delta_{n_1,0}\operatorname{Re}[(if)^n]\big)N_{(n)}^2. \quad (15.14)$$

15.2 Absence of branching corrections to inclusive spectrum

Let us study the single particle inclusive spectrum. In Lecture 10 we saw that in the pole approximation the inclusive spectrum is given by the Mueller–Kancheli diagram (15.1). Take now a two-reggeon branching. Since I need to register a particle in the central region, the quasi-elastic cut (15.2a) does not contribute. In the cross section, the screening correction diagram (15.2b) was twice as large as the graph with two cut reggeons, (15.2c). However, when both ladders are cut, I can take the necessary particle from either of them, and hence, this imaginary part enters with a factor 2 the inclusive spectrum:

$$0 \times 2 \ - 8 \ + 2 \times 4 = 0$$

The meaning of an inclusive spectrum is the multiplicity multiplied by the cross section:

$$\int f(\eta)\,d\eta = \sum_n n\sigma_n \equiv \bar{n}\sigma.$$

Recall how we arrived at this: the phase volume of k identical particles contains $1/k!$. Fixing the momentum of one of the particles, I have for the remaining ones $\frac{1}{(n-1)!}\prod_{i=1}^{n-1}dk_i$.

Let us show that there will never be any corrections to the inclusive spectrum in the central region. As we already know, n-reggeon branching with $n_1 > 0$ cut reggeons contributes to the cross section as

$$2\operatorname{Im}F_{n_1}^{(n)} = C_{n_1}^n(-1)^{n-n_1}(2\operatorname{Im}f)^n. \quad (15.15)$$

Calculating the inclusive spectrum, I have to multiply this expression by n_1, and to sum over n_1 in order to obtain the total contribution of the branching:

$$\delta f^{(n)} \propto \sum_{n_1=1}^{n} n_1 \cdot C_n^{n_1}(-1)^{n-n_1} = \sum_{n_1=1}^{n} \left[n - (n - n_1) \right] \cdot C_n^{n_1}(-1)^{n-n_1}$$

$$= \left\{ n(1+\kappa)^n - \kappa \frac{\partial}{\partial \kappa}(1+\kappa)^n \right\}_{\kappa=-1} = n \cdot (1+\kappa)^{n-1}\bigg|_{\kappa=-1}.$$

Since $n \geq 2$ (we do not consider a pole), the total contribution of an arbitrary non-enhanced branching to the inclusive spectrum equals zero.

Let us consider a more complicated diagram. The diagram is integrated over rapidities η_1, η_2 at which the reggeons interact, while we are looking for a particle with a certain rapidity η. Depending on the order of the rapidities, we have three situations:
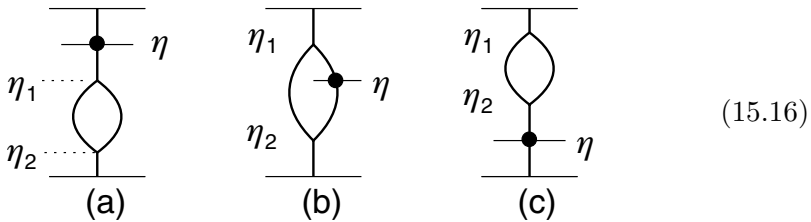
$$(15.16)$$

(1) $\eta_2 < \eta_1 < \eta$, (15.16) graph (a), or $\eta < \eta_2 < \eta_1$ (c). There are no cancellations; we have a correction to the inclusive spectrum.

(2) $\eta_1 > \eta > \eta_2$, (15.16) graph (b). In this region the contributions of one and two cut regions cancel; $\delta f(\eta) = 0$.

This consideration shows that I can draw any reggeon corrections from above or from below of the registered particle, but never embrace the point η. Summing up the total set of such diagrams leads, obviously, to replacing the Green functions, G, of the bare pomeron pole by the *exact* Green functions, $\mathbf{G}$:

$$\frac{d\sigma}{d\eta \, d^2\mathbf{k}_\perp} = g_1 \mathbf{G}(\xi - \eta)\varphi(k_\perp^2)\mathbf{G}(\eta)g_2. \qquad (15.17)$$

15.2.1 Shape of the inclusive spectrum

How do reggeon branchings affect the shape of the inclusive spectrum?

Weak coupling. In the pomeron pole approximation, the inclusive spectrum is flat in the central rapidity region, $f(\eta) = \text{const}$. Reggeon loops
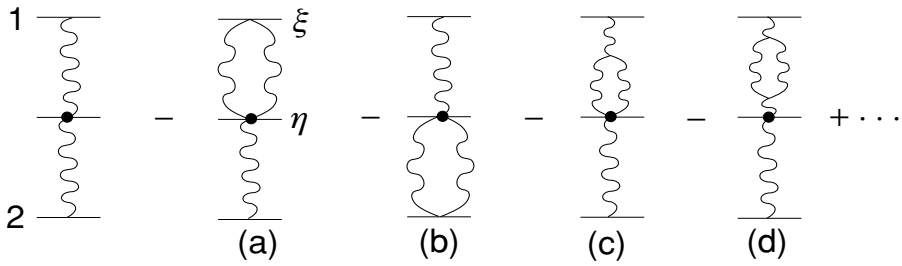
Fig. 15.3   One-loop corrections to inclusive spectrum (weak coupling).

provide sub-asymptotic corrections to the plateau. In addition to the corrections to the top and bottom pomeron propagators (Fig. 15.3(d)), we may take the triggered particle right from the three-reggeon vertex r as shown in Fig. 15.3(a–c). Let us evaluate the first correction term, Fig. 15.3(a):

$$f(\eta, \mathbf{k}^2) = g_1 \varphi(\mathbf{k}^2) g_2 - \int \frac{d^2\mathbf{k}'}{(2\pi)^2} N_1 \cdot \mathrm{e}^{-2\alpha'\mathbf{k}'^2(\xi-\eta)} \tilde{\psi}(\mathbf{k}, \mathbf{k}') \cdot g_2 + \cdots ,$$

where $\mathbf{k}'$ is the transverse momentum flowing through the reggeon loop. Since the rapidity interval $\xi - \eta$ is large, $\mathbf{k}'$ is small, and we may replace $\tilde{\psi}(\mathbf{k}, \mathbf{k}') \simeq \tilde{\psi}(\mathbf{k}, 0) \Rightarrow \psi(\mathbf{k}^2)$.

$$f(\eta, \mathbf{k}^2) \simeq g_1 g_2 \varphi(\mathbf{k}^2) - \frac{N_1 g_2}{4\pi} \frac{\psi(\mathbf{k}^2)}{2\alpha' \cdot (\xi - \eta)} + \cdots . \tag{15.18}$$

In the weak coupling regime the vertex vanishes, $r \propto \omega \sim \mathbf{k}^2$. Therefore in Fig. 15.3(c,d) the pomeron propagators neighbouring the loop cancel, so that these graphs reduce, in fact, to Fig. 15.3(a), modifying the function ψ in (15.18).

We obtain the distribution

$$f(\eta, \mathbf{k}^2) \simeq g_1 g_2 \varphi(k_\perp) - \frac{C_1(\mathbf{k}^2)}{\xi - \eta} - \frac{C_2(\mathbf{k}^2)}{\eta}, \tag{15.19}$$

where we added the contribution of the symmetric graph (b). We conclude that the plateau must have a *positive curvature*.

Strong coupling.   In the strong coupling regime this property is expressed in a much more manifest way. Here essential multi-reggeon corrections are contained in the Green function itself, $G(\xi) \propto \xi^\mu$, so that the inclusive

spectrum,

$$f(\xi; \eta, \mathbf{k}^2) \simeq g_1 G(\xi - \eta) \varphi(\mathbf{k}^2) G(\eta) g_2,$$

increases with energy, as does the total cross section. It make sense to measure the inclusive cross section in units of σ_{tot}:

$$\phi(\xi; \eta, \mathbf{k}^2) \equiv \sigma_{\text{tot}}^{-1}(\xi) \cdot f(\xi; \eta, \mathbf{k}^2), \quad \sigma_{\text{tot}}(\xi) \propto G(\xi) \propto \xi^\mu;$$

$$\phi(\xi; \eta, \mathbf{k}^2) \propto \frac{G(\xi - \eta) G(\eta)}{G(\xi)} \propto \xi^\mu \cdot z^\mu (1 - z)^\mu, \quad z \equiv \frac{\eta}{\xi}.$$

Unlike the parton model, where the system was 'forgetting' about its boundaries, here the situation is different. There is now neither a 'zeroth approximation', as in the weak-coupling case, nor an asymptotic plateau. The Feynman scaling is broken: the probability of finding a particle depends seriously not only on its place in the rapidity but also on the total energy.

Let us calculate the total multiplicity:

$$\int_0^\xi d\eta \int d^2 \mathbf{k}\, \phi(\xi; \eta, \mathbf{k}^2) \equiv \bar{n}(\xi) \propto \xi^{\mu+1} \cdot \int_0^1 dx\, x^\mu (1 - x)^\mu.$$

The mean multiplicity has increased significantly – where did this come from? In the strong coupling case enhanced multi-reggeon diagrams are essential. This fact alone makes it evident that $\bar{n}$ must grow.

Indeed, recall the distribution for topological cross sections, σ_n. From Fig. 15.1 for multiplicity fluctuations due to the two-reggeon branching, it is not obvious, a priori, in what direction the average value moves, to the left or to the right. But, the more complicated branchings are included, the more the number of cuts grows compared with the number of uncut reggeons, resulting in the multiplicity increase.

From the space–time picture, in strong coupling our 'ladder' consists often of a few ladders of normal density tied together. Hence, in the course of the interaction a larger number of particles is 'shaken off'.

15.3 Two-particle correlations

To study multiplicity fluctuations, not only average quantities can be investigated but also the correlations of particles which allow us to find the dispersion of the multiplicity distribution. Let us construct the cross section for inclusive production of two particles with momenta k_1, k_2,

$$f(k_1, k_2) = \sum_n \frac{1}{(n - 2)!} \int d\Gamma_{n-2} |F_n(k_1, k_2; q_1, \dots, q_{n-2})|^2,$$

where

$$dΓ_{n-2} = \prod_{i=1}^{n-2} dΓ(q_i), \quad dΓ(q) = \frac{d^3q}{2q_0(2π)^3},$$

is the phase space volume for $n-2$ unregistered particles with momenta q_i.

If we now integrate the double differential distribution f over momenta k_1, k_2 of the triggered particles, we obtain the second multiplicity moment:

$$\int dΓ(k_1)\, dΓ(k_2) f(k_1, k_2) = \sum_n \frac{1}{(n-2)!} \int dΓ_n |F|^2$$

$$= \sum_n n(n-1) \int \frac{dΓ_n}{n!}\, |F|^2 = \sum_n n(n-1)σ_n \equiv \overline{n(n-1)}σ_{\text{tot}}. \quad (15.20)$$

Recall that the integral of a *single particle* inclusive cross section gives the average multiplicity,

$$\int dΓ(k_1) f(k_1) = \bar{n}σ_{\text{tot}}.$$

Constructing the *correlation function*

$$φ(k_1, k_2) \equiv \frac{f(k_1, k_2)}{σ_{\text{tot}}} - \frac{f(k_1)f(k_2)}{σ_{\text{tot}}^2}, \quad (15.21)$$

we have

$$\int dΓ_1\, dΓ_2\, φ(k_1, k_2) = \overline{n(n-1)} - \bar{n}^2 = \overline{n^2} - \bar{n}^2 - \bar{n}. \quad (15.22)$$

If particles are produced independently then, obviously,

$$φ(k_1, k_2) = 0 \quad \Longrightarrow \quad \overline{n^2} - \bar{n}^2 = \bar{n},$$

which is a property of the Poisson distribution. Hence, $φ \neq 0$ describes the deviation from the independent emission.

If rapidities $η_1$, $η_2$ are close, nothing definite can be said. If, however, the relative rapidity $η_1 - η_2$ is large, and both particles are far away from the fragmentation regions ($η_2 \gg 1$, $ξ - η_1 \gg 1$), in zeroth approximation we can draw a pole picture and see that $φ(η_1, η_2) = 0$. In an approximation without corrections, pomeron exchange gives rise to a homogeneous

Poisson distribution:

$$f(\eta_1, \mathbf{k}_1; \eta_2, \mathbf{k}_2) = \quad = g_1 \varphi(k_1^2) \varphi(k_2^2) g_2. \qquad (15.23)$$

We take now two-reggeon branching:

$$\qquad (15.24)$$

What will we get from more complicated branchings? Again, we take an n-reggeon branching diagram, cut n_1 reggeons, and choose two particles from them:

$$2 \operatorname{Im} F_{n_1}^{(n)} = C_n^{n_1} \cdot (-1)^{n-n_1} (2 \operatorname{Im} f)^n \cdot \left[\frac{n_1(n_1 - 1)}{2} + n_1 \right], \qquad (15.25)$$

where $n_1(n_1 - 1)/2$ is the number of ways to select two particles from different reggeons, and n_1 from the same reggeon. We know, however, that $\sum_{n_1} n_1 \cdot 2 \operatorname{Im} F$ gives zero, cf. (15.24); hence,

$$n_1(n_1 - 1) \implies \frac{\partial^2}{\partial x^2} (1-x)^n \bigg|_{x=1},$$

and only the branching $n = 2$ contributes. A general statement can be verified: non-enhanced branchings up to the nth order contribute to the cross section of the production of n particles.

In order to generalize this result for enhanced branchings, one has to be somewhat careful. Indeed, for the standard cancellation to take place, we have to make sure that the reggeon interaction vertices do not depend on the way the diagrams are cut, e.g. the vertex λ in (15.26),

$$\qquad (15.26)$$

As a result, a very important picture emerges: in the full set of reggeon diagrams for two-particle inclusive spectrum any interactions between the reggeons are possible except those in the interval between the rapidities η_2 and η_1 of the triggered particles.

In the weak coupling regime one can verify that the correction (15.24) *broadens* the multiplicity distribution of particles compared to the Poisson distribution.

To analyse the multiplicity fluctuation pattern in the case of the strong coupling is a much more difficult task. To see qualitatively, what is taking place let us consider the simplest diagram with the scaling Green functions, $G(\xi) \propto \xi^\mu$ substituted for the pomeron poles in (15.23). For the double inclusive distribution we then have

$$\phi(k_1, k_2) = \frac{G(\xi-\eta_1)G(\eta_1-\eta_2)G(\eta_2)}{G(\xi)} - \frac{G(\xi-\eta_1)G(\eta_1)}{G(\xi)} \cdot \frac{G(\xi-\eta_2)G(\eta_2)}{G(\xi)}.$$

Keeping $x_1 = \eta_1/\xi$ and $x_2 = \eta_2/\xi$ fixed, both terms behave as $\xi^{2\mu}$. Now we calculate the integral (15.22), extracting the overall ξ-dependence:

$$\xi^{-2\mu-2} \cdot \int d\Gamma_1 \, d\Gamma_2 \, \phi(k_1, k_2)$$

$$\propto \int dx_1 \, dx_2 (1-x_1)^\mu |x_1 - x_2|^\mu x_2^\mu - \left(\int dy (1-y)^\mu y^\mu \right)^2$$

$$= 2 \int_0^1 dx_1 (1-x_1)^\mu x_1^{2\mu+1} \int_0^1 dy (1-y)^\mu y^\mu - \left(\int_0^1 dy (1-y)^\mu y^\mu \right)^2$$

$$= \int_0^1 dy (1-y)^\mu y^\mu \cdot \left[2B(\mu+1, 2\mu+2) - B(\mu+1, \mu+1) \right] < 0, \quad (15.27)$$

where $B(a,b) = \Gamma(a)\Gamma(b)/\Gamma(a+b)$. The problem is that the combination of the B-functions in the square brackets is *negative* ($\mu > 0$). This means that the distribution became *narrower* than the poissonic one, which is rather strange. Moreover, for a sufficiently large ξ (15.27) would violate the mathematical fact that $\langle n^2 \rangle - \langle n \rangle^2 \geq 0$. Consequently, the branching corrections must be significant. In any case, there is a large positive correlation between particles in the strong coupling scenario.

15.4 How to tame fluctuations

We return to the discussion of fluctuations.

The simplest one is just the elastic scattering. There is an interesting class of fluctuations of a similar nature, which we considered in Lecture 10
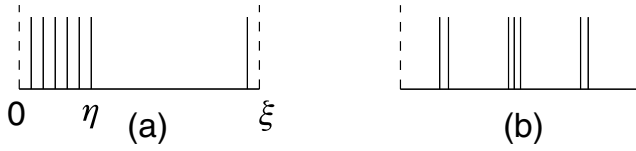
Fig. 15.4   Inelastic diffraction (a) and an event with large rapidity gaps (b).

when we discussed the inconsistency of the Regge-pole approximation. These fluctuations are characterized by large intervals in the rapidity distribution of produced hadrons, as shown in Fig. 15.4.

15.4.1 High-mass inelastic diffraction: triple-reggeon limit

The first process, Fig. 15.4(a), is simple to measure. Indeed, to make sure that there are no other fast particles, it is sufficient to observe a particle with an energy very close to the initial one. (There can be no uniform plateau when we register too energetic a particle in the final state.) This is a correlation forced by the energy conservation.

The invariant mass of particles produced on the side of the target is

$$M^2 = (k_1 + k_2 + \cdots + k_n)^2 \simeq m^2 \, e^\eta, \qquad (15.28)$$

where η can be equated with the rapidity of the fastest particle k_1 in the bunch $(k_{10} \gg k_{20} \gg \cdots \gg k_{n0} \sim m)$, cf. (10.32b). In the kinematics of Fig. 15.4(a), the mass is small compared to the total energy, $M^2 \ll s$. At the same time, it can be large in absolute terms, $M^2 \gg m^2$, so that the condition $\xi \gg \eta \gg 1$ can be satisfied. Then the cross section transforms into the three-reggeon picture as shown in Fig. 15.5. Hence, selecting a particle with a large momentum, I virtually measure the three-reggeon vertex directly. This is just the same vertex r that enters the reggeon diagrams, since, as we know, it does not change when the diagram is cut.
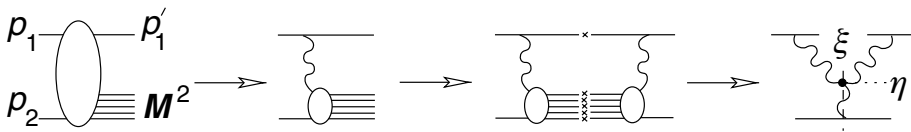
Fig. 15.5   Inclusive spectrum in the triple-reggeon limit.

Let us see that the vertex r, indeed, has to go to zero, as this follows from the reggeon field theory. We calculated this diagram in Lecture 10, see (10.35):

$$
\begin{aligned}
d\sigma_{3\mathbf{P}} \;\propto\; & \frac{1}{s}\frac{d^3p_1'}{2E_1'} \cdot g_1^2(\mathbf{q}_\perp^2)\,r(\mathbf{q}_\perp^2)\,g_2(0) \\[4pt]
& \cdot \left| i\frac{s}{M^2}G(\xi-\eta,\mathbf{q}_\perp^2)\right|^2 \cdot \left[M^2 G(\eta,0)\right] \\[4pt]
& \sim d^2\mathbf{q}_\perp\, d\eta\, g_1^2 r g_2 \cdot \mathrm{e}^{-2\alpha'\mathbf{q}_\perp^2(\xi-\eta)}; \quad d\eta = \frac{dx}{1-x}.
\end{aligned}
\tag{15.29}
$$

Here x is the energy fraction carried by the fast registered particle which has to be chosen in the interval $m^2/s \ll 1-x \ll 1$ in order to satisfy the conditions of applicability of the reggeon approximation, $\xi - \eta \gg 1$, $\eta \gg 1$ (see (10.32)).

Strictly speaking, the inclusive spectrum has the meaning of cross section *weighted* by particle multiplicity, $n \cdot \sigma$. However, when measuring $x > \frac{1}{2}$, I am sure there may be only one particle with such a large energy in the event. Consequently, by measuring the inclusive particle yield in the three-reggeon kinematics we measure not multiplicity, but directly the contribution of the total cross section.

How large is this contribution? We have to integrate (15.29) over a large rapidity interval, η up to ξ. If the cone did not shrink, $\alpha' = 0$, we would have $\mathrm{e}^{-2\alpha'\mathbf{q}^2(\xi-\eta)} = 1$, and

$$
\int^\xi d\eta \int d^2\mathbf{q}_\perp \frac{d\sigma_{3\mathbf{P}}}{d\eta\, d^2\mathbf{q}_\perp} \;\sim\; r \cdot \xi,
\tag{15.30}
$$

i.e. an infinitely increasing with energy partial contribution to the cross section! This is, essentially, the same contradiction as the one we faced when we discussed the black disc model, $A = s \cdot F(t)$, in Lecture 6. But even taking account of $\alpha' \neq 0$ the result is still unacceptable:

$$
\sigma_{3\mathbf{P}} = \int^\xi d\eta \int d^2\mathbf{q}_\perp \frac{d\sigma_{3\mathbf{P}}}{d\eta\, d^2\mathbf{q}_\perp} \sim \int_0^{\xi-\mathrm{const}} \frac{d\eta}{\alpha'(\xi-\eta)} \;\sim\; \ln\xi.
\tag{15.31}
$$

Although growing much slower with s that in (15.30), $\sigma_{3\mathbf{P}}$ eventually takes over $\sigma_{\mathrm{tot}} = \mathrm{const}$. To avoid the contradiction, we have to have, in accord with the reggeon field theory consideration, see (14.27),

$$
r(\mathbf{q}_\perp) \;=\; c\,\mathbf{q}_\perp^2, \quad \text{for } \mathbf{q}\to 0,
\tag{15.32}
$$

in which case

$$
\int d^2\mathbf{q}_\perp \frac{d\sigma_{3\mathbf{P}}}{d^2\mathbf{q}_\perp} \;\sim\; \frac{d\eta}{|\xi-\eta|^2}, \quad \text{and} \quad \sigma_{3\mathbf{P}} = \mathcal{O}(1).
$$
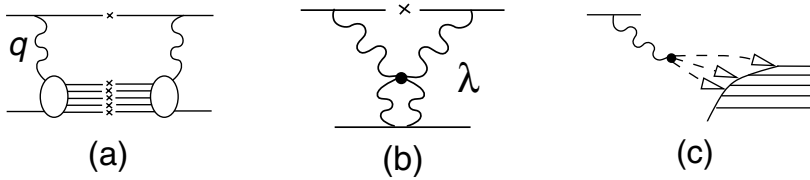
Fig. 15.6

In the *strong coupling* regime, the reggeon–reggeon interaction vertices also effectively vanish at small $\mathbf{q}_\perp$.

15.4.2 Vanishing reggeon–reggeon vertices

Let us turn to the discussion of an important question.

We see from (15.32) that the scattering cross section vanishes in the *forward direction*, $\mathbf{q}_\perp \to 0$. This is a strong conclusion which has to have serious consequences.

Indeed, is it not strange that the total cross section of the inelastic diffraction processes in Fig. 15.6(a) has to turn into zero for $\mathbf{q}_\perp = 0$? (Strictly speaking, there should be no *pomeron pole* in the bottom part of Fig. 15.6(a), while something like Fig. 15.6(b) could, in principle, be there.) If I draw a ladder, would not the expression be positively definite? One can imagine playing on the non-locality of the vertex in attempt to effectively *screen* it, by integrating over the place where the reggeon is attached, as shown in Fig. 15.6(c). As we will see shortly, this is not an easy thing to do.

Nevertheless, let us suppose that we managed somehow to force the three-pomeron vertex vanish for the forward scattering, $r(0) = 0$. Then a two-pomeron branching in Fig. 15.6(b) gives the leading contribution to the inclusive cross section which, obviously, has to be positive. But we know that the total imaginary part of the branching diagram is *negative*: $2 - 8 + 4 = -2$. To avoid the contradiction, the four-pomeron vertex λ also has to be put to zero at $\mathbf{q} = 0$.

15.4.3 Multi-particle production with large rapidity gaps

One arrives at the same conclusion, $\lambda \to 0$, by considering another curious fluctuation, when there is a large number of 'holes' in the distribution in rapidity, see Fig. 15.4(b) above. (Historically, this was the first example of a fluctuation that has led to the contradiction.)
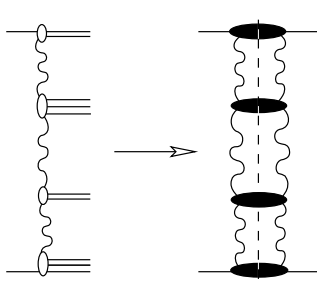
The corresponding cross section can be calculated in different ways. In the j-plane representation one easily gets

$$\sigma(\omega) = \left\{ \text{\raisebox{-1ex}{}} \right\} \propto \ \lambda^2 \ln \omega^{-1}. \qquad (15.33)$$

Summing up two-reggeon loops,

$$\sum_{n=1}^{\infty} \lambda^n \ln^n \omega^{-1} = \frac{\lambda \ln \omega^{-1}}{1 - \lambda \ln \omega^{-1}},$$

we get a pole *to the right* from unity. Although the loop diagram (15.33) itself amounts to a relatively small correction,

$$\sigma(\xi) \sim \int \frac{d\omega}{2\pi i} \ln \omega^{-1} \, \mathrm{e}^{\omega \xi} \ \sim \ \xi^{-1};$$

its repetition in the t-channel gives rise to a very strong exponential enhancement, $\exp(\omega_0 \xi)$, $\omega_0 > 0$. This contradiction (the existence of a subprocess whose cross section grows faster than the total one) requires, once again, to have $\lambda(0) = 0$.

15.4.4 Fluctuations in the weak and strong coupling regimes

In the weak coupling case the s-channel unitarity imposes very serious restrictions on the theory. The conditions $r(0) = \lambda(0) = 0$ are needed to make sure that large fluctuations would not ruin the stationary uniform rapidity distribution that characterizes the pomeron. In the language of the reggeon field theory, these are actually the requirements that keep our system away from the critical point.

The case of strong coupling does not contain contradictions, either in the '3**P** limit', or for multiple large rapidity gaps.

Given the σ_{tot} increasing with energy, the large deviations from the scaling solution (14.22) turn out to be (relatively) suppressed. The screening of dangerous fluctuations is achieved here by summing diagrams with 'long' *reggeons* substituted for the dashed lines in Fig. 15.6(c). This tells us (as strange as it may sound) that it is *easier* to verify the strong-coupling scenario than the weak coupling one.

In the first case we have a reggeon field theory (RFT) at our disposal. We can plug in a bare pomeron pole and carry out the analysis* (although we do not know a priori whether there is a small parameter in the theory, we can at least try to calculate things within this hypothesis).

In the weak coupling, the vanishing of the vertex in Fig. 15.6(c) has to be demonstrated at the level of *particles* (hadrons) rather than reggeons. Therefore, in order to check the weak coupling regime, detailed knowledge of the true theory of hadrons is necessary. This makes a world of a difference: while the *reggeons* enable us to carry out calculations, at least in principle, *hadrons* do not: we do not have a theory of strongly interacting *hadrons*.

The weak coupling corresponds to a rather simple physical picture:

(1) total cross sections are asymptotically constant;

(2) there is a uniform rapidity distribution;

(3) the multiplicity grows logarithmically with energy;

(4) fluctuations in particle production are relatively rare; and

(5) branching corrections to the leading pole approximation are small.

In contrast with that, the strong coupling regime has a rather complicated structure. Here:

(1) the total cross sections increase, $\sigma_{\text{tot}}(s) \sim \ln^\nu s$ (with $0 < \nu \le 2$);

(2) there is no asymptotic particle density;

(3) no factorization;

(4) not much is left of the initial pole; branchings are 100% important; and

(5) the leading approximation for the reggeon Green function G can be fixed only roughly, in a 'dimensional sense'.

These two versions are different also in the 'microscopic' language.

In the *weak coupling* there exists the asymptotic parton wave function of a fast hadron, which ensures *factorization* of high-energy interactions. This wave function is characterized by a finite rapidity density of particles and is boost invariant.

In the *strong coupling* case the systems never forgets about its initial energy. Long-range correlations are omnipresent, and the parton content

---

* Indeed, an example is known based on a definite relation between the bare vertex r and the pole trajectory $\alpha(t)$, in which the strong-coupling solution does emerge (ed.).

of colliding hadrons keeps growing with the energy of the interaction. One might say, there is a specific Lorentz frame characterizing each collision.

On the physics side, the first reggeon field theory scenario looks more elegant. However, from the point of view of a pure theory – summing up the pictures – the impression is just the opposite.

Indeed, the strong coupling can be obtained directly from the diagrams. Meanwhile, the weak coupling calls for additional requirements ($r(0) = \lambda(0) = 0$) which, in terms of diagrams, do not follow from anything: they are just necessary to impose in order to preserve the s-channel unitarity.

15.5 Weak coupling: vanishing pomeron–particle vertices

The study of the s-channel picture of particle production is very efficient in understanding the conditions for the self-consistency of the theory. We see that for the consistency of the weak coupling regime, rather strong additional conditions must be satisfied namely, that the reggeon interaction vertices r and λ vanish in the $\mathbf{q}_\perp \to 0$ limit. But if they do, what will remain? Generally speaking, it is not so easy to set something to zero by hand in a field theory; will this not result, e.g. in all cross sections becoming zero too?

The hypothesis $\sigma_{\text{tot}} \to$ const looks rather attractive. So, we will recall the main steps of the analysis of fluctuations we have carried above, to see what are the consequences of the weak coupling conditions $r(0) = \lambda(0) = 0$.

15.5.1 π-meson production vertex

Let us fix a large η value and keep increasing $\xi - \eta$. Taking into account all corrections to the pole on the bottom part of the three-reggeon graph,

$$(15.34)$$

we arrive at the so-called reggeon–particle scattering amplitude:

$$(15.35)$$

We are interested in the forward scattering ($t = 0$). This amplitude can be studied in terms of the partial wave, $f(\omega, \mathbf{k})$. The limit $\eta \to \infty$ corresponds to $\omega \to 0$, in which limit the vertex r goes to zero. The pomeron contribution to the scattering block disappears, and there remain only

non-pole contributions (branching corrections). This means that the reggeon–particle amplitude (15.35) *decreases* with the growth of energy, η. Let us recall, however, the s-channel meaning of the branchings. The total cross section for the scattering of the pomeron $\mathbf{P}$ on a particle, $\sigma_{\text{tot}}^{(\mathbf{P})}$,

$$\sigma_{\text{tot}}^{(\mathbf{P})} = \sum_n \sigma_n,$$

is a sum of topological cross sections, σ_n, with the production of a given number of hadrons. We have discussed that the branchings lead to the appearance of processes with particle multiplicity smaller ($n < \bar{n}(\eta)$) and larger than the average ($n > \bar{n}(\eta)$), as well as to negative corrections to the pole term. Now that the leading term has disappeared, these corrections dominate the answer and would result in the *negative cross section* for the processes with the average multiplicity, $\sigma_{n\sim\bar{n}} < 0$.

We conclude that λ in (15.35) must also go to zero. The necessity of the vanishing of the four-reggeon vertex followed also from the consideration of multiplicity fluctuations with multiple large rapidity gaps. From that consideration it was not clear, however, under what specific conditions λ has to be zero.

The three-reggeon vertex r on the r.h.s. of (15.35) is zero when the momentum $\mathbf{k}$, transferred along the pomeron, vanishes (and $\omega = 0$, corresponding to the $\eta \to \infty$ limit). This makes it evident that we have to have $\lambda = 0$ as soon as $\mathbf{k} = 0$, independently of the value of the momentum $\mathbf{k}'$ in the lower part of the branching graph.

Let us construct the four-reggeon vertex λ in the ω-representation:

$$\lambda(\omega; \mathbf{k}, \mathbf{k}') = \int d\eta \, e^{-\omega\eta} \, \text{Im} \, A_{\mathbf{PP}}(\eta; \mathbf{k}, \mathbf{k}'), \qquad (15.36)$$

where $A_{\mathbf{PP}}$ is the $\mathbf{PP}$ scattering amplitude. The integral on the r.h.s. of (15.36) must vanish at $\omega = 0$, $\mathbf{k} = 0$. However, by virtue of the s-channel unitarity condition (optical theorem for $\mathbf{PP}$ scattering), the imaginary part of the forward amplitude can be represented as a sum of cross sections,

$$0 = \lambda(0; \mathbf{0}, \mathbf{k}') = \int d\eta \, \text{Im} \, A_{\mathbf{PP}}(\eta; \mathbf{0}, \mathbf{k}') = \int d\eta \sum_n . \qquad (15.37a)$$

We integrate a sum of the amplitudes squared. Hence, we come to the conclusion that *each* of these amplitudes has to be zero at $\mathbf{k} = 0$:

$$\mathbf{n} = 0 \quad \text{when } \mathbf{k}=0, \text{ for any } \eta \text{ and } \mathbf{k}', \qquad (15.37\text{b})$$

identically for all energies. This is actually what we saw in the case of the multi-gap events, with only one addition: to have $\lambda = 0$ it is in fact sufficient to put to zero the transverse momentum of *one* of the reggeons.

Take a particular case $n = 2$, and consider the production of two pions:

$$\equiv 0 \ = \ \sum_{\mathbf{R}} \ \mathbf{R} \qquad \pi, \qquad (15.37\text{c})$$

where we have expanded the amplitude over Regge poles $\mathbf{R}$ (by choosing π we exclude from the sum the vacuum pole $\mathbf{P}$). But different reggeons have different energy behaviour, hence *each term* of the sum is zero.

Next, the Regge-pole amplitudes factorize; therefore from (15.37c) we conclude that *each* $\mathbf{PR}\pi$ *vertex* vanishes in this point,

$$= 0. \qquad (15.37\text{d})$$

Now, let us continue this 'zero' in the virtuality $t' = -\mathbf{k}'^2$ of the reggeon $\mathbf{R}$ to the point $t' = m_b^2$, to obtain a particle–particle–pomeron amplitude,

$$a \ \underline{\quad\quad} \ b \ = 0. \qquad (15.37\text{e})$$

15.5.2 Goodbye pomeron?

We arrived at a fantastic result: the transition amplitude $b \to a$ must vanish with the transferred transverse momentum, $\mathbf{k}_\perp \to 0$, independently of the type of the target! Moreover, if we take $a = b$, (15.37e) would mean that the forward elastic amplitude is zero, and so is its imaginary part, and the total cross section. The pomeron does not hook onto any hadron, and therefore does not exist!

We learned that the high mass inelastic diffraction of the target hadron does not contain the pomeron pole when the projectile particle scatters *forward*, $r(\mathbf{k}_\perp = 0) = 0$, and were hoping that as a result the amplitude (15.34) would slowly decrease with the increase of $\eta \simeq \ln M^2$. However, having carried the reggeon logic through the consecutive steps (15.37), we seem to have arrived at a totally bizarre conclusion.

15.6 How to rescue a pomeron

We must address the two cases contained in (15.37e) separately:

- $b \neq a$ – a surprising prediction;

- $b = a$ – a catastrophe; the end of the pomeron hypothesis.

In the first case we deal with an inelastic process, and no formal objection can be raised against vanishing of inelastic amplitudes on a pomeron.

In order to rescue the *elastic* scattering, $b = a$, we could have the following situation: the genuine vertex, strictly speaking, could be *singular* at $m_a = m_b$. The singularity which prevents the elastic vertex from becoming zero could be of the form
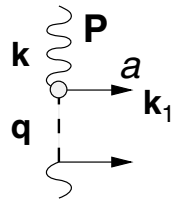
$$\gamma(\mathbf{k}, \mathbf{q}) \;\propto\; \frac{2(\mathbf{k}_\perp \mathbf{q}_\perp)}{m_a^2 + \mathbf{k}_{1\perp}^2}. \tag{15.38}$$

(Such an object – the *transverse mass* of the produced particle, $m_a^2 + \mathbf{k}_{1\perp}^2$, – always enters the reggeon cross sections.) Let us introduce $t = -\mathbf{q}^2$,

$$\frac{2(\mathbf{k}_\perp \mathbf{q}_\perp)}{m_a^2 + (\mathbf{q} + \mathbf{k})_\perp^2} = \frac{2(\mathbf{k}_\perp \mathbf{q}_\perp)}{m_a^2 - t_2 + 2(\mathbf{q}_\perp \mathbf{k}_\perp) + \mathbf{k}_\perp^2},$$

and analytically continue the amplitude into the point $t = m_b^2 > 0$, where the dashed reggeon line in (15.38) represents a particle b:

$$\frac{2(\mathbf{k}_\perp \mathbf{q}_\perp)}{m_a^2 - m_b^2 + 2(\mathbf{k}_\perp \mathbf{q}_\perp) + \mathbf{k}_\perp^2} \;\xrightarrow{\mathbf{k}_\perp \to 0}\; \left\{ \begin{array}{ll} 1, & a = b \\ 0, & a \neq b \end{array} \right\}. \tag{15.39}$$

Hence, formally, our aim can be achieved. This is, however, not a real proof, although this may be more than just a mathematical trick. In fact, it is exactly what happens in quantum electrodynamics.

15.6.1 Vanishing of the vertex in quantum electrodynamics

Consider some inelastic QED process, for example photon conversion into an $e^+ e^-$ pair in the external electromagnetic field:

$$= (+e) + (-e) = 0.$$

The incoming particle creates a current which is scattered on the field. If $\mathbf{k}_\perp$ is small, this field is almost homogeneous and therefore interacts only with the *integral* of the current, i.e. with the total electric charge. But the charge is conserved; it does not change when the system fluctuates (e.g. $\gamma \to e^+ e^- \to \gamma$). As a result, the scattering on a *homogeneous* electromagnetic field ($\mathbf{k}_\perp \to 0$) does not alter the internal state of the projectile.

How can this be seen mathematically? Writing the Weizsäcker–Williams formula, we get just the singularity that we invented in (15.39).

Take an arbitrary process in which an incident particle a transforms into an object (a system of particles) with the total momentum p_b and invariant mass $p_b^2 = m_b^2 \geq m_a^2$. A stationary field does not transfer energy, $A_\mu(k) \propto \delta_{\mu,0}\delta(k_0)$, and we have

$$k_0 = 0;$$
$$p_b^2 = (p_a + k)^2 = m_a^2 - 2p_z k_z - \mathbf{k}_\perp^2 - k_z^2. \qquad (15.40)$$

When the energy is large, $p_{a0} \simeq p_{az} \equiv p$, the longitudinal momentum absorbed by the field becomes small,

$$k_z = \sqrt{p^2 - (m_b^2 - m_a^2 + \mathbf{k}_\perp^2)} - p \simeq -\frac{m_b^2 - m_a^2 + \mathbf{k}_\perp^2}{2p}, \qquad (15.41)$$

and the transferred momentum is transversal, $k^2 \simeq -\mathbf{k}_\perp^2$.

M_μ is the matrix element of the sub-process $a + \gamma(k) \to b$ shown by the grey blob in (15.40). It must satisfy the current conservation condition,

$$k^\mu M_\mu = k_0 M_0 - k_z M_z - (\mathbf{k}_\perp \mathbf{M}_\perp) = 0, \qquad (15.42)$$

from which we derive

$$M_z = -\frac{(\mathbf{k}_\perp \mathbf{M}_\perp)}{k_z} \simeq 2p \cdot \frac{(\mathbf{k}_\perp \mathbf{M}_\perp)}{m_b^2 - m_a^2 + \mathbf{k}_\perp^2} \simeq M_0,$$

where we used (15.41). Finally, for the amplitude of the process we obtain

$$A^\mu M_\mu \propto M_0 \propto \frac{(\mathbf{k}_\perp \mathbf{M}_\perp)}{m_b^2 - m_a^2 + \mathbf{k}_\perp^2}, \qquad (15.43)$$

were we have exploited the fact that in a relativistic situation, $M_0 \simeq M_z$ ($M_0 - M_z = \mathcal{O}(1/p) \to 0$).

This is precisely the structure of the vertex we are seeking to rescue the pomeron. With $\mathbf{k}_\perp \to 0$, it goes to zero for $m_a \neq m_b$ but stays finite for the elastic scattering, $a = b$ (in which case $\mathbf{M}_\perp \propto \mathbf{k}_\perp$, for lack of any other transverse vector in the problem).

We could discuss this phenomenon in the language of Lorentz-invariant form factors. If the object b has no internal structure (is characterized

only by its total four-momentum p_b), we may write

$$M_\mu(p_a, p_b) = \Gamma_1(k^2)(p_a + p_b)_\mu + \Gamma_2(k^2)(p_a - p_b)_\mu.$$

The condition (15.42) gives $\Gamma_1(m_a^2 - m_b^2) + \Gamma_2 k^2 = 0$, and we obtain

$$a = b: \; M_\mu = \Gamma_1(k^2)(p_1 + p_2)_\mu,$$

$$a \neq b: \; M_\mu = \Gamma_2(k^2) \left[\frac{k^2}{m_b^2 - m_a^2}(p_1 + p_2)_\mu + k_\mu \right]; \quad \Gamma_i(k^2) \xrightarrow{k^2 \to 0} \text{const.}$$

In the latter case the high-energy inelastic transition vanishes in the forward direction, $M_0(a \to b) \propto \mathbf{k}_\perp^2 \cdot p + \mathcal{O}(1/p)$, while the elastic amplitude is finite, $M_0(a \to a) \simeq e \cdot 2p$.

Hence, although this example looks somewhat artificial, it demonstrates that the solution we are looking for may exist. Actually, this is not an argument in favour of the pomeron, since in quantum electrodynamics we have a conservation law in the game (that of electric charge).

Nevertheless, the elastic scattering in the reggeon problem is not zero either, and there is a reason for that.

15.6.2 Diffraction on a broad potential (deuteron)

Let us study another example.

In Lecture 12 we discussed the diffraction on a large size target. We considered the scattering of a deuteron off the external field of size R (Fig. 15.7) and wrote the transition amplitude from the initial state i to the final state k:

$$f_{ik} \sim \int d^3 r_{12} \, d^2 \boldsymbol{\rho}_c \, \psi_k^*(r_{12}) \left[e^{2i\delta(\boldsymbol{\rho}_1) + 2i\delta(\boldsymbol{\rho}_2)} - 1 \right] \psi_i(r_{12}). \qquad (15.44a)$$

When the spread of the potential is much larger than the internal size of the projectile, $R \gg r_D$, in the scattering phases $\delta(\boldsymbol{\rho}_1)$, $\delta(\boldsymbol{\rho}_2)$ we can neglect the separation $\boldsymbol{\rho}_{12}$ between the proton and neutron inside the
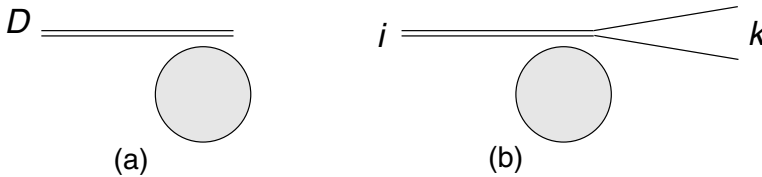
Fig. 15.7

deuteron, $\boldsymbol{\rho}_1 = \boldsymbol{\rho}_c + \frac{1}{2}\boldsymbol{\rho}_{12} \simeq \boldsymbol{\rho}_2 = \boldsymbol{\rho}_c - \frac{1}{2}\boldsymbol{\rho}_{12} \simeq \boldsymbol{\rho}_c$, to obtain

$$f_{ik} \sim \underbrace{\int d^3 r_{12}\, \psi_k^*(r_{12})\psi_i(r_{12})}_{\delta_{ik}} \cdot \int d^2\boldsymbol{\rho}_c \left[e^{4i\delta(\rho_c)} - 1 \right]. \qquad (15.44b)$$

Thus, while the *elastic* process ($i = k$) goes, the amplitude becomes zero when $i \neq k$ that is for scattering with excitation – inelastic channel, Fig. 15.7(b).

We have established a correspondence of these formulae with 'pictures'. Recall the representation for the scattering matrix element that we have used in order to translate (15.44) in the language of the diagrams:

$$S_1 S_2 - 1 = (S_1 - 1) + (S_2 - 1) + (S_1 - 1)(S_2 - 1). \qquad (15.45)$$

Consider two concrete cases.

First we take $i = \psi_D$, $k = \psi_D$, corresponding to the elastic scattering:


$$\neq 0. \qquad (15.46)$$
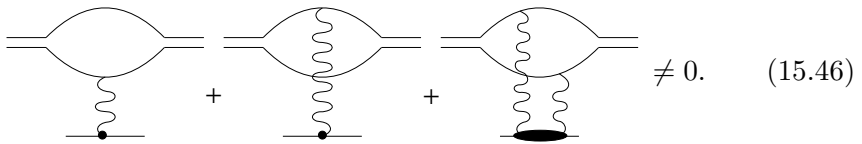
Now let us draw the *decay*, when ψ_k is the wave function of the continuous spectrum, $k = (n, p)$. What is the corresponding graphical representation? The wave function of the produced n, p can be written as

$$\psi_k = e^{ik\cdot r_{12}} + \psi'_{n,p}, \qquad (15.47)$$

where $\psi'_{n,p}$ is an addition due to the interaction between n and p in the final state. Let us insert it in the integral (15.44b) for the transition amplitude f_{ik} represented in the form of (15.45).

The free propagation gives

$$(15.48a)$$
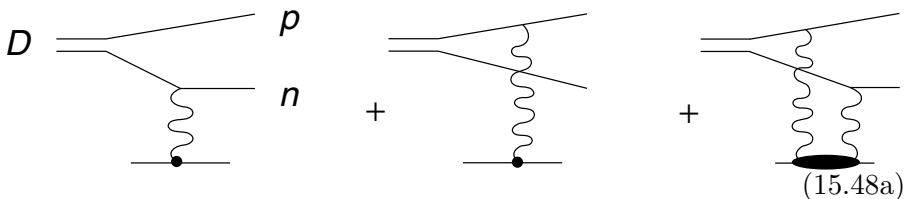
Owing to the additional term ψ'_{np} in (15.47), after the interaction with the target there is an interaction between the two outgoing nucleons:

$$(15.48b)$$
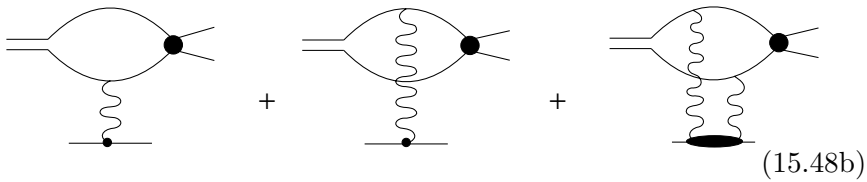
Having drawn the diagrams, we may hope that this picture can be applied in a more general context (not only to a deuteron).

From the properties of the wave function, (15.44b), we know that the dissociation amplitude is zero at $\mathbf{k}_\perp = 0$. How does this happen in terms of diagrams? The mechanism of the cancellation between the graphs (15.48a) and (15.48b) turns out to be very similar to the case of a conserved current.

The final state interaction amplitude shown by black circles in (15.48b) may be rather complicated. However, I can expand it over intermediate states, and I know that at $\mathbf{k} = 0$ only one of them would survive namely, the *pole term* corresponding to D. Then the sum of the diagrams (15.48) reduces to two graphs displayed in Fig. 15.8, where the dashed block symbolizes the sum of the amplitudes for scattering of the two nucleons off the target.
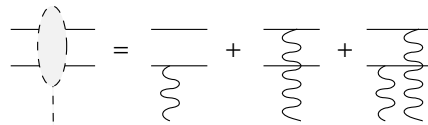
The two graphs of Fig. 15.8 must cancel one another in the $\mathbf{k} \to 0$ limit. How is this possible?

The second graph (Fig. 15.8(b)) describes forward scattering of the deuteron (followed by its dissociation); therefore its amplitude is proportional to $\sigma_{\text{tot}}(D)$ – the cross section of deuteron interaction with the target.
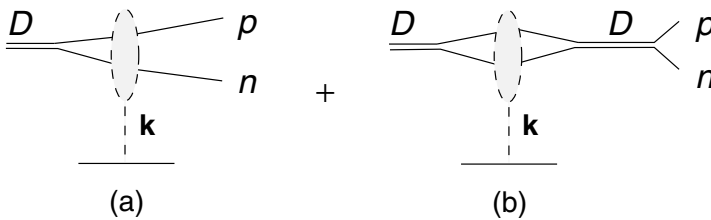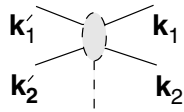

Fig. 15.8   (a) $D \to pn$ dissociation followed by interaction of nucleons with the target, (15.48a); (b) D pole in the final state pn interaction amplitude, (15.48b).

The first graph (Fig. 15.8a) can be also expressed via the total cross section, this time, of the $p + n$ pair. Indeed, if the potential is broad, we may neglect, once again, its dependence on $\boldsymbol{\rho}_{12}$ and approximate $V(\boldsymbol{\rho}_1, \boldsymbol{\rho}_2) \simeq V(\boldsymbol{\rho}_c)$:

$$
\text{(diagram)} \quad = \int d^2\boldsymbol{\rho}_{12}\, e^{i(\mathbf{k}_{12} - \mathbf{k}'_{12}) \cdot \boldsymbol{\rho}_{12}} \cdot V(\boldsymbol{\rho}_1, \boldsymbol{\rho}_2) \;\propto\; \delta(\mathbf{k}_{12} - \mathbf{k}'_{12}).
$$

(15.49)

The internal state momenta $\mathbf{k}'_i$ coincide with the final momenta $\mathbf{k}_i$; the proton and neutron scatter *forward*, and the amplitude yields $\sigma_{\text{tot}}(np)$.

So it becomes clear that for the cancellation to take place, the equality of the cross sections is necessary,

$$
\sigma_{\text{tot}}(D) \;=\; \sigma_{\text{tot}}(np). \tag{15.50}
$$

This relation obviously holds in our model: both D and pn interaction amplitudes are determined by the standard formula (15.44a), and in case of scattering on a large target it is irrelevant, whether p and n are flying separately, or together, inside D. If we were to carry out the real calculation, we would see that the normalization factors conspire in such a way that (15.50) turns out to be not only *necessary* but also *sufficient* for the cancellation of graphs (Fig. 15.8), which describe pn and D interacting with the target, correspondingly.

Let us demonstrate how it happens, by applying the Feynman rules to the forward $a \to b$ amplitude in the external field:

$$
\text{(diagrams)} \;=\; \gamma \frac{1}{m_b^2 - p^2} \sigma_{\text{tot}}^{(b)} + \sigma_{\text{tot}}^{(a)} \frac{1}{m_a^2 - p^2} \gamma. \quad (15.51)
$$

γ is the transition amplitude between the states ($a = D$, $b = p + n$). The virtuality p^2 of the intermediate state (shown by a thick line) is defined differently in the two diagrams (15.51). Namely, $p^2 = m_a^2$ in the first term (state a is on the mass shell), and $p^2 = m_b^2$ in the second (on-mass-shell state b). We immediately see that as soon as $\sigma_{\text{tot}}(a) = \sigma_{\text{tot}}(b)$, the amplitude vanishes (the propagators do their job properly).

This example shows that inelastic transitions $a \to b$ can indeed be zero at $\mathbf{k}_\perp \to 0$ if the interactions in the initial and final states cancel. To make it possible, the particles a and b must *interact identically* with the target, have to have *equal total cross sections*.

In the considered case of scattering on a large target this is true not only for the total cross sections, $\sigma_{\text{tot}}(a) = \sigma_{\text{tot}}(b)$, but even in a more subtle sense: scattering does not lead to a redistribution of momenta in the continuous spectrum, see (15.49).

15.7 Vanishing of forward inelastic diffraction in RFT

How could one discuss this situation without appealing to the quantum-mechanical deuteron analogy?

Let us take our hypothesis that the amplitudes of inelastic processes vanish when the transverse momentum $\mathbf{k}$ transferred along the pomeron goes to zero,

$$a \quad \overset{b}{\underset{\mathbf{k}=0 \;\; \mathrm{P}}{\bullet}} \quad c \quad = 0, \tag{15.52}$$

and ask ourselves how to derive consequences of this condition, not knowing the theory of hadron interactions?

15.7.1 'Sharp screening' in RFT

I put to zero not a constant but a function of the pair energy (invariant mass) s_{bc}. As any other amplitude, (15.52) has singularities. In particular, it may have a pole at $s_{bc} = m_a^2$. It is not difficult to write the pole term explicitly:

$$a \quad \overset{a \quad b}{\underset{\mathbf{k}=0 \;\; \mathrm{P}}{\bullet}} \times \quad c \qquad \propto \sigma_{\mathrm{tot}}(a) \neq 0. \tag{15.53}$$

This contribution to the amplitude is non-zero, since it is proportional to $\sigma_{\mathrm{tot}}(a)$. How could a function having a pole be zero? There may be other intermediate states too,

$$a \quad \overset{d \quad b}{\underset{\mathbf{k}=0 \;\; \mathrm{P}}{\bullet}} \times \quad c \qquad \propto \sigma(a \to d) = 0. \tag{15.54}$$

However, by our hypothesis, the $a \to d$ transition on the pomeron is forbidden, and therefore no other states contribute to the imaginary part (the discontinuity over s_{bc}). Have we not 'killed' the hypothesis (15.52)? The answer is 'no', and for a subtle reason.

The amplitude (15.52) is a four-point function, having many variables. Usually, after making use of the Lorentz invariance, we talk about two independent variables and, correspondingly, two independent imaginary parts (discontinuities). But a Regge amplitude is *not* Lorentz invariant; it depends on the direction of the collision. We are concerned with $\mathbf{k}_\perp = 0$.

If I set to zero the *total* four-vector $k_\mu = 0$, the amplitude (15.52) would turn into a three-point function. The latter is fully determined by the particle masses, $A(m_a^2, m_b^2, m_c^2)$, and has no free variables left.

If I take $(k_\mu)^2 = 0$, this is one condition, equivalent to fixing the mass of one external line of the four-point amplitude; two independent variables are at our disposal.

Setting $\mathbf{k}_\perp = 0$ means, however, *two* conditions, not one. Therefore, the amplitude (15.52) at this point possesses only *one* independent variable. As a result, when studying the s_{bc} imaginary part, we have to take into consideration simultaneously discontinuities over s_{ab} and s_{ac}! We can draw two additional simple graphs straight away:

$$\tag{15.55}$$

All three amplitudes have poles at the same point. Suppose, this were the whole answer. Then the condition (15.52) would read

$$\sigma_{\text{tot}}(a) \;=\; \sigma_{\text{tot}}(b) + \sigma_{\text{tot}}(c).$$

But this is nonsense.

In the deuteron story it was not like that. For the system of two nucleons we had $\sigma(pn) = 2\pi R^2$, and not $\sigma(pn) = 2 \times 2\pi R^2$.

What is missing in (15.55)? The screening correction. It is this additional term that saved the day in the deuteron case:

$$\implies \quad \sigma(pn) = 4\pi R^2 - 2\pi R^2 = 2\pi R^2. \tag{15.56}$$

The battle is not won yet. Indeed, each of three diagrams in (15.55) has a *pole*, while the screening graph (15.56) does not seem to have one. But it has to have a pole in order to participate in the cancellation we are looking for.

Actually, there *is* a pole which emerges in a very peculiar way.

On a broad potential, the double interaction is 'sharp'. As I have stressed above, there emerges $\delta(\mathbf{k}' - \mathbf{k})$: momenta of particles in the intermediate state coincide with the final state ones, $\mathbf{k}'_i = \mathbf{k}_i$ $(i = 1, 2)$. The energy denominator of the intermediate state peaks, producing the pole.
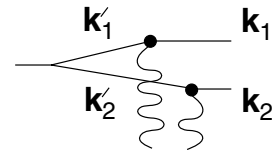
Before we turn to the question whether such a phenomenon appears in the reggeon problem, let me make a remark. As in the deuteron case, see

(15.50), the self-consistency condition (15.37e) will imply

$$a \underset{\mathbf{P}\underset{\mathbf{k}=0}{\big\}}{\overline{}} b = 0 \quad \Longrightarrow \quad \sigma_{\mathrm{tot}}(a) = \sigma_{\mathrm{tot}}(b). \tag{15.57}$$

Cross sections of different objects (hadrons) that can turn into one another on the pomeron (having the same quantum numbers) must be asymptotically equal.

15.7.2 The essence of reggeon screening

We have to discuss whether we can obtain a necessary screening contribution in the reggeon framework. Let us draw the corresponding reggeon diagram,
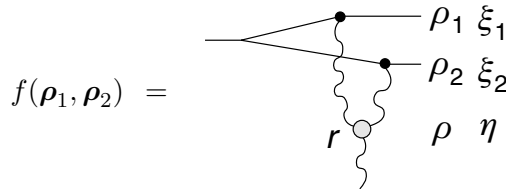
and calculate it presuming $r(0) \neq 0$, for a start. Formally speaking, we would not expect a branching diagram to have a pole in ω; in other words, we would expect it to be small in the high-energy limit, $\xi \to \infty$.

In the impact parameter language,

$$f(\boldsymbol{\rho}_1, \boldsymbol{\rho}_2) = r \int d^2\boldsymbol{\rho}\, d\eta\, G(\boldsymbol{\rho}_1 - \boldsymbol{\rho}, \xi_1 - \eta) G(\boldsymbol{\rho}_2 - \boldsymbol{\rho}, \xi_2 - \eta) G(\boldsymbol{\rho}, \eta). \tag{15.58}$$

This is the contribution to the amplitude from the three-pomeron diagram. Since the Green function G is Gaussian in $\boldsymbol{\rho}$, see (12.19), the integral can be easily calculated. But even without calculation we can answer the question whether there will remain the dependence on the relative distance $\boldsymbol{\rho}_{12}$.

What sort of a problem is this? The rapidities $\xi - \eta$ and η play the rôle of time in the diffusion process. We deal with a probability for two objects, emerging from points $\boldsymbol{\rho}_1$ and $\boldsymbol{\rho}_2$, to meet after time $\xi - \eta$ in the point $\boldsymbol{\rho}$, and keep propagating, stuck together. The integral over η and $\boldsymbol{\rho}$ means that I am looking for the total probability of such a meeting anywhere in the 'space–time'. The point is, in the two-dimensional space this *always happens*.

The brownian motion formula, $\langle \boldsymbol{\rho}^2 \rangle \sim T$, means that the size of the region where the diffusing object can be found at time T, increases linearly with T. On the other hand, the path length is also proportional to T.

This tells us that our object, typically, visits *each point* inside the disc of increasing radius. Indeed, the probability to be found in a given point $\boldsymbol{\rho}$ any time *before* T,
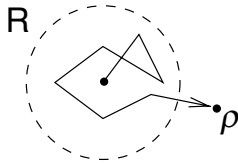
$$w(T, \boldsymbol{\rho}^2) \sim \int_0^T dt \frac{\exp(-\boldsymbol{\rho}^2/t)}{t} \sim \ln\frac{T}{\boldsymbol{\rho}^2},$$

grows with the time elapsed. It makes it look plausible that the probability for the two objects to meet (anywhere, some time) will grow too: for sufficiently large $T \gg \boldsymbol{\rho}_{12}^2$, the collision occurs inevitably, irrespectively of the size of the initial separation. Let us look at the formula to see if our expectation materializes.

Substituting in (15.58) $\boldsymbol{\rho}_{1(2)} = \boldsymbol{\rho}_c \pm \frac{1}{2}\boldsymbol{\rho}_{12}$,

$$f \sim \int \frac{d^2\boldsymbol{\rho}\, d\eta}{(\xi-\eta)^2} \exp\left(-\frac{(\boldsymbol{\rho}_c - \boldsymbol{\rho})^2}{2\alpha'(\xi-\eta)} - \frac{\boldsymbol{\rho}_{12}^2}{8\alpha'(\xi-\eta)}\right) \times \frac{1}{\eta} \exp\left(-\frac{\boldsymbol{\rho}^2}{4\alpha'\eta}\right).$$

We are interested in the forward amplitude, $\int d^2\boldsymbol{\rho}_c \exp(i\mathbf{k}\cdot\boldsymbol{\rho}_c)$ at $\mathbf{k} = 0$. Integrals over $\boldsymbol{\rho}_c$ and $\boldsymbol{\rho}$ compensate two nomalization factors, and we are left with

$$f(\boldsymbol{\rho}_{12}^2, \mathbf{k} = 0) \sim \int_0^\xi \frac{d\eta}{\xi-\eta} \exp\left(-\frac{\boldsymbol{\rho}_{12}^2}{8\alpha'(\xi-\eta)}\right) \simeq \ln\frac{8\alpha'\xi}{\boldsymbol{\rho}_{12}^2}.$$

The dependence on $\boldsymbol{\rho}_{12}$ drops out in the dominant piece of the amplitude, $f \sim \ln\xi$, and therefore the integration over $\boldsymbol{\rho}_{12}$ produces the delta-function contribution $\delta(\mathbf{k} - \mathbf{k}')$ that we are looking for.

Well, I deceived you, of course. If I substitute in (15.58) the vanishing **PPP** vertex, $r(0) = 0$ (as I should have done) this graph is simply small.

15.7.3 Bare and renormalized three-pomeron vertices

We are discussing whether particles screen each other when they interact via pomeron exchange.

What is the difference between **P** and a simply large target? On one hand, the pomeron resembles a large target because its radius grows with energy as $\ln s$. On the other hand, the cross section on a large target is also very large $\sigma \sim R^2$, while in the pomeron case the disc becomes more and more transparent with the increase of energy.

The fact that screening corrections are large on a large target is essentially trivial; as soon as one particle hits the target, so does the second one inside the projectile. If I had $r \neq 0$, this situation could reproduce itself in the pomeron problem, owing to the blackening of the disc that
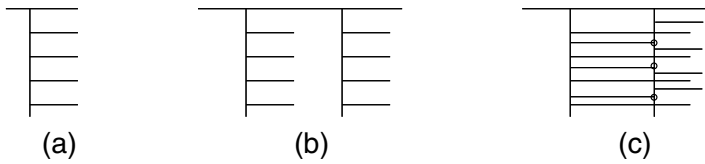
Fig. 15.9   (a) Image of a bare pole; (b) branching; (c) interacting ladders.

corresponds to the 'true pole'. However, if $r(0) = 0$, then the pomeron disc remains transparent and does not provide the necessary sharp screening.

But what is a 'true pole'?

We need to reflect upon the meaning of a 'pole' and 'branching'. If there is an interaction between 'ladders', a new mixed coherent state emerges, representing the 'true pomeron' (Fig. 15.9(c)). Cutting through such an object, I would not necessarily find large fluctuations.

And what would be a branching then?

It describes a situation when two such objects (the true poles) do not interact during a long period. The weak coupling condition, $r \to 0$, means that such long-living fluctuations are not frequent, i.e. the uniform rapidity distribution is quasi-stable – it does not fluctuate much. From this perspective, the vertex r is responsible for *deviations* from the stable asymptotic distribution. This vertex function r has to go to zero.

When discussing various reggeon branching issues, we drew diagrams and used to write the same letter r for the three-pomeron vertex. However, there were essentially different quantities!

In particular, in the case of a deuteron, the ladders surely do not overlap for a long time since p and n inside the deuteron are far apart. Many diffusion step are necessary in order for the ladders to meet. On average, $\alpha'(\xi - \eta) \simeq \langle \boldsymbol{\rho}_{12}^2 \rangle \sim r_D^2$. Thus, during a *very long* 'time' $r_D^2/\alpha' \gg 1$ they typically do not mix together and develop independently.[†]

The proper size of the deuteron is an external factor. Thus, the properties of the deuteron wave function impose themselves on the reggeon theory.

The vertex r that governs the magnitude of fluctuations around the stationary distribution I would call *renormalized*, r_{ren}. It is this vertex that has to vanish in the forward kinematics, for the sake of self-consistency of the weak-coupling pomeron theory.

[†]   There is a possibility for p, n to be initially close, but it has a small probability (ed.).

At the same time, the quantity r that enters the deuteron scattering problem I would treat as a *bare* reggeon interaction vertex, $r_{\text{bare}} \to \text{const}$, because in this concrete case a (seldom fluctuating) asymptotic coherent parton distribution does not have enough time to be formed (and hardly ever will, at any energies imaginable).

Constructing the theory of interacting reggeons, I would have to start from a bare vertex, $r_{\text{bare}} = \text{const}$, and then (provided I really knew how to calculate things) to *demonstrate* that the renormalized one indeed vanishes, $r_{\text{ren}}(\mathbf{k} \to 0) \to 0$. The analysis of the triple-reggeon limit in (15.58) was actually a step in this direction; by calculating such three-reggeon graph we were calculating in fact the *true* (renormalized) deuteron–pomeron vertex via the bare **PPP** constant r_{bare}.
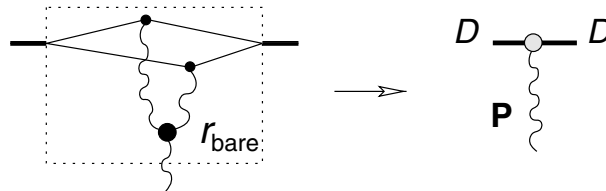
Whether this program can be realized in reality remains unclear; the full understanding is lacking of how, essentially, the renormalization of the pomeron constants takes place.

With somewhat less certainty, we can make the statement (15.57) even stronger; total interaction cross sections of all particles (and not only those having identical quantum numbers) must tend to one and the same constant in the limit of asymptotically high energies.

15.8 All σ_{tot} are asymptotically equal?

In order for the screening phenomenon to be independent of the specificity of the state, it is necessary to be able to calculate the screening correction graph (see, e.g. (15.56)) in a universal manner via reggeons (and not particles!).

Suppose that in the consistency condition (15.57),

we take the particle b to be a composite object, $b = c + d$. Then the interaction of this object with the target I will represent as a sum of three

contributions:

$$\sigma_b = \sigma_{(cd)} \;\; = \qquad \qquad + \qquad \qquad + \qquad \qquad$$

where the interaction block V is universal, not depending on the types of the participating particles. In terms of pomeron–particle interaction constants, this is a non-linear relation,

$$g_b = g_c + g_d + g_c g_d \cdot V. \tag{15.59}$$

But c and d can be chosen differently; a hadron can be 'composed' in multiple different ways. A proton, for example: $p = n + \pi^+ = \Delta^{++} + \pi^-$, etc. Therefore, the only solution (15.59) admits is $g_c = g_d = g_b$.

Thus, having supposed that the high-energy screening is determined by the pure reggeon physics, we come to the conclusion

$$\sigma_{\text{tot}}^{(p)}(s \to \infty) = \sigma_{\text{tot}}^{(\pi)}(\infty) = \sigma_{\text{tot}}^{(D)}(\infty) = \sigma_{\text{tot}}^{(He^4)}(\infty) = \;\cdots$$

Is it really so weird to have the interaction cross sections of all hadrons with a given target to be asymptotically equal?

In order for this to happen in reality, one would need, of course, grandiose colliding energies, such that the reggeon interaction processes are fully developed: $\alpha \ln s \gg R_h^2$, the Regge radius of the pomeron *much larger* than the proper radii of the projectile hadrons.

Parton clouds belonging to the constituents inside the hadron must all mix together, resulting in the coherent universal parton distribution whose density no longer depends on the type of the incident hadron. When this limit is reached, the interaction cross section in the centre-of-mass frame of the initial particles A and B is expressed in a universal way, via the interaction cross section of slow ('wee') partons.

In the framework of the parton picture, the hypotheses which guarantees an asymptotic equality of *all* cross sections looks rather natural. It presumes that, due to the fact that the hadron interaction is *strong*, such a universal distribution is reached, eventually, with the unit probability, and does not depend on the nature of colliding objects.